Operational Parameters of a Diesel Engine Running on Diesel–Rapeseed Oil–Methanol–Iso-Butanol Blends

Jakub Čedík [1,*] , Martin Pexa [1] , Michal Holúbek [1], Jaroslav Mrázek [1], Hardikk Valera [2] and Avinash Kumar Agarwal [2]

1   Department for Quality and Dependability of Machines, Faculty of Engineering, Czech University of Life Sciences Prague, Kamýcká 129, 165 21 Prague, Czech Republic; pexa@tf.czu.cz (M.P.); holubekm@tf.czu.cz (M.H.); mrazekjaroslav@tf.czu.cz (J.M.)
2   Engine Research Laboratory, Department of Mechanical Engineering, Indian Institute of Technology Kanpur, Kanpur 208016, India; hardikk@iitk.ac.in (H.V.); akag@iitk.ac.in (A.K.A.)
*   Correspondence: cedikj@tf.czu.cz; Tel.: +420-224383321

Academic Editors: Marcis Jansons and Timo Kikas

Abstract: This contribution focuses on utilizing blended biofuels of rapeseed oil and methanol with diesel. Rapeseed is one of the most cultivated energy crops in Europe, and its purpose in the blends is to increase the bio-content in test fuels. The purpose of methanol in the blends is to increase bio-content and compensate for the higher viscosity of the rapeseed oil. As methanol is almost insoluble in diesel and rapeseed oil, iso-butanol is used as a co-solvent. The fuel blends were tested in volumetric concentrations of diesel/rapeseed oil/methanol/iso-butanol 60/30/5/5, 50/30/10/10, and 50/10/20/20. Diesel was used as a reference. The measurements were performed on a turbocharged diesel engine Zetor 1204, loaded using the power-takeoff shaft of the Zetor Forterra 8641 tractor. In this paper, the effect of the blended fuels on performance parameters, engine efficiency, production of soot particles, and regulated and unregulated emissions are monitored and analyzed. It was found that engine power decreased by up to 27%, efficiency decreased by up to 5.5% at full engine load, emissions of NO_X increased by up to 21.9% at 50% engine load, and production of soot particles decreased; however, the mean size of the particles was smaller.

Keywords: diesel engine; fuel consumption; harmful emissions; biofuels; rapeseed oil; methanol; iso-butanol; diesel

1. Introduction

The utilization of alternative fuels can decrease greenhouse gasses (GHG) emissions and reduce the dependence on imported crude oil products [1–5]. Alternative fuel usage primarily results in significant price savings compared to conventional fuels (gasoline and diesel). The sectors contributing most to the global economy's progress include the agriculture sector. Therefore, it becomes necessary to explore the possibilities of alternative fuel usage in the agriculture sector. It is also one of the significant energy-consuming sectors responsible for substantial GHG emissions from human activities [6]. Compression ignition (CI) engines are mainly used to power the equipment in the agriculture sector. Alternative fuel families are large enough, covering families made of different combinations of carbon-hydrogen (C–H) molecules such as alcohols, ethers, vegetable oils, etc. [7]. The alcohol family has several members, where the hydroxyl group (-OH) is attached to the carbon molecule, such as methanol (CH_3-OH), ethanol (CH_3-CH_2-OH), propanol (CH_3-CH_2-CH_2-OH), butanol (CH_3-CH_2-CH_2-CH_2-OH), etc. Propanol, butanol, and other higher carbon content alcohols have structural isomers depending on different positions of the -OH group. Ether family includes dimethyl ether (CH_3-O-CH_3), diethyl ether (CH_3-CH_2-O-CH_2-CH_3), methyl ethyl ether (CH_3-O-CH_2-CH_3), etc. Vegetable oils include soybean oil, sesame oil, grapeseed oil, sunflower oil, rapeseed oil, etc. Currently, pure plant oil (PPO) usage, which includes corn, peanut, coconut, olive, jatropha [8], rapeseed, karanja [9],

and cottonseed [10], is gaining momentum in European Union (EU) countries. Several researchers reported the possibility of PPO usage in the pure or blended form in diesel engines [11–16]. Much work has been done in rapeseed oil production, quality testing, and its usage in agriculture tractors and heat power generation [17–21]. Rapeseed oil usage seems to be beneficial because (i) the source of rapeseed oil is renewable; (ii) it has a high energy density (7% lower than mineral diesel); and (iii) physiochemical properties are pretty similar to mineral diesel [22].

Rapeseed is a flowering member of the Brassicaceae family, cultivated to extract the oil [23,24]. It contains a considerable amount of erucic acid and glucosinolates with 8.1% moisture, 3.7% ash, 20.3% crude fiber, 45.2% oil, and 18.7% protein [25]. It is only second to soybean oil in the oilseed category based on growing global demand and production. Its combustion in the diesel engine faces cold starting issues; thus, it warrants preheating. It has a lower cetane number and higher boiling point temperature than mineral diesel. It is, however, ~10 to ~20 times more viscous than rapeseed methyl esters and mineral diesel, respectively. Viscosity plays a vital role in diesel engines since it affects the atomization of fuels. Higher viscosity increases the period of the spray atomization process, thereby negatively affecting the in-cylinder combustion process [26]. Previous studies show that vegetable oils cause operational issues due to nonvolatility, higher viscosity, and higher density [27–31]. Therefore, developing a novel approach to use the advantageous rapeseed oil in the existing engines becomes necessary. It is possible to modify the fuel properties using different methods such as transesterification [32–34], hydrotreatment [35,36], heating [37], and ternary or quaternary blends with low viscosity fuels such as diesel, biodiesel, and alcohols [21,38–41]. The transesterification process is the best technology from an economic point of view because of low pressure and temperature conditions, resulting in maximum product yield [42]. This process is also known as alcoholises because alcohols are used with oils in the presence of a catalyst for biodiesel production [43]. The transesterification, hydrotreatment, or preheating require additional energy, however, blending the vegetable oil with diesel and suitable alcohols with low viscosity, such as methanol and iso-butanol, does not require any additional energy for fuel processing, and it is investigated as a promising alternative solution [5,21,44].

Methanol, as the simplest alcohol (CH_3OH), can be produced from different feedstocks, including municipal waste and biomass, coal and other fossil sources, CO_2 captured from the atmosphere, etc. [4,45–47]. In addition, it can be easily stored and transported in liquid form at standard atmospheric conditions [48,49]. It has ~50% inherent oxygen in its molecular mass, which affects its fuel properties [50]. However, methanol has several disadvantages that limit its usage as a fuel admixture in diesel. The main issues are the low cetane number [51], low calorific value, high latent heat of evaporation [52] combined with its high volatility, and poor solubility in diesel [53–56]. Poor solubility attributes to the opposite nature of diesel and methanol, i.e., polar and nonpolar, limiting the methanol blending in diesel to 10–25% [4,7,53]. It is hygroscopic and absorbs atmospheric water vapour, which causes phase separation problems with mineral diesel [57,58]. The addition of co-solvents can improve the low solubility issues of methanol [59]. Researchers used several different co-solvents/additives, such as dimethyl ether, diethyl ether, hexanol [60,61] or dodecanol [62,63]; iso-alcohols such as iso-propanol, iso-butanol, or iso-octanol; and their products, such as iso-octyl nitrate [62,64] or fatty acids such as oleic acid to improve the solubility. In addition, the solubility of methanol in the fuel blend can be enhanced by the addition of biodiesel (fatty acid methyl esters—FAME) [39,65] or the use of FAME as a base fuel [66]. However, the low viscosity of methanol could become a boon for rapeseed oil usage. Furthermore, several researchers recommended that 100% rapeseed oil is inappropriate in an unmodified diesel engine [17,22].

On the other side, researchers are also exploring the possibility of using iso-butanol in a diesel engine. It is an isomer of butanol, having four carbon molecules. It can be produced by fermentation of sugarcane/corn. In addition, it can be produced from cellulose fermentation [67], but these production routes compete with food crops. However, it

can also be made from the electromicrobial transformation of CO_2 and biochemical pathways [68]. Molecular mass wise, it has 21.5% inherent oxygen in its chemical compound, which attracted researchers to test it as a fuel for powering engines. It has a lower energy density (33.1 MJ/kg) than mineral diesel [69]. Several researchers tested iso-butanol-diesel blends as a fuel [70–75]; however, its application as an additive/emulsifier was also investigated [76]. It is reasonably clear that due to the favourable properties of iso-butanol, researchers used it in engines.

Although a few attempts have been made to use rapeseed oil for existing diesel engines in blends using additives, the combination of methanol–rapeseed oil–iso-butanol has not been investigated. Furthermore, the areas of unregulated emissions and particulate characteristics remain unexplored. Therefore, this article aims to investigate experimentally the effect of diesel–rapeseed oil–methanol–iso-butanol blends on the CI engine performance parameters, regulated and unregulated emissions, and soot generation.

2. Materials and Methods

2.1. Test Fuels

Blends of diesel, rapeseed oil, methanol, and iso-butanol as a co-solvent were used as test fuels. According to EN 590 [77], the reference fuel was diesel with no bio-components (D100). The blended fuels were tested in the following volumetric concentrations:

- 60% diesel, 30% rapeseed oil, 5% methanol, 5% iso-butanol—M5;
- 50% diesel, 30% rapeseed oil, 10% methanol, 10% iso-butanol—M10;
- 50% diesel, 10% rapeseed oil, 20% methanol, 20% iso-butanol—M20.

Specifications of the test fuels and their base components are shown in Table 1. The kinematic viscosity and density of the fuels were determined using the Stabinger Viscometer SVM 3000 from Anton Paar GmbH (measurement accuracy < 1%, repeatability = 0.1%). As seen from Table 1, the kinematic viscosity of M10 and M20 fulfil the standard for diesel (EN 590) [77], and the viscosity of M5 fulfils standard EN 14214 for biodiesel [78]. The calorific values of the base fuels were determined using the isoperibol calorimeter LECO AC600 (range 23.1–57.5 MJ/kg for a 0.35 g sample, accuracy 0.1% RSD) according to ČSN DIN 51900-1 [79] and ČSN DIN 51900-2 [80]. Carbon, hydrogen, and oxygen content of methanol and iso-butanol were calculated based on atom masses of the atoms in its molecule; for the fuel blends, the content of C, H, and O was calculated based on mass concentration of these base components, determined based on measured densities and volumetric concentrations.

Table 1. Test fuel specifications and their components.

Fuel	Kinematic Viscosity at 40 °C (mm^2 s^{-1})	Density at 15 °C (kg m^{-3})	Calorific Value (MJ kg^{-1})	Cetane Number	Latent Heat of Evaporation (kJ kg^{-1})	Carbon Content (%wt)	Hydrogen Content (%wt)	Oxygen Content (%wt)
D100	2.587	835	43.2	50 [1]	250 [2]	87 [1]	13	0
Rapeseed oil	35.697	905.33	37.1	41.6 [3]	-	78.1 [4]	11.9 [4]	10 [4]
Methanol	0.563	797.57	19.6	<5 [5]	1180 [6]	37.5	12.6	49.9
Iso-butanol	2.729	807.17	33.1	<15 [7]	566 [7]	64.8	13.6	21.6
M5	4.505	855.9	39.7	-	-	80.8	12.7	6.5
M10	4.204	853.6	38.1	-	-	77.4	12.7	9.9
M20	2.214	836.25	36	-	-	72.2	12.9	14.9

[1] Data obtained from [77], [2] Data obtained from [81,82], [3] Data obtained from [83], [4] Data obtained from [84], [5] Data obtained from [45], [6] Data obtained from [53], [7] Data obtained from [85].

During the measurements, mechanical stirring was applied to prevent phase separation. When left undisturbed, the phase separation occurred in M10 and M20 blends despite iso-butanol use as co-solvent. The mixed fuels without stirring can be seen in Figure 1. It is evident that while for M10, a relatively small amount of alcohol content separated, for M20, the phase separation was strong. Almost the entire alcohol content separated from the rest of the blend. M10 and M20 after the application of stirring are shown in Figure 2.

For M5, no visible phase separation occurred, as can be seen in Figure 1. The tested fuels were mixed and used at room temperature (~25 °C).
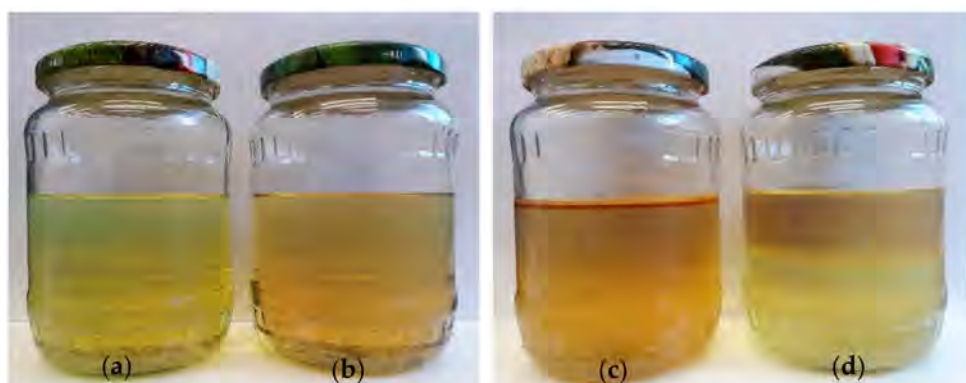

Figure 1. Test fuel blends: (**a**) D100, (**b**) M5, (**c**) M10, (**d**) M20.
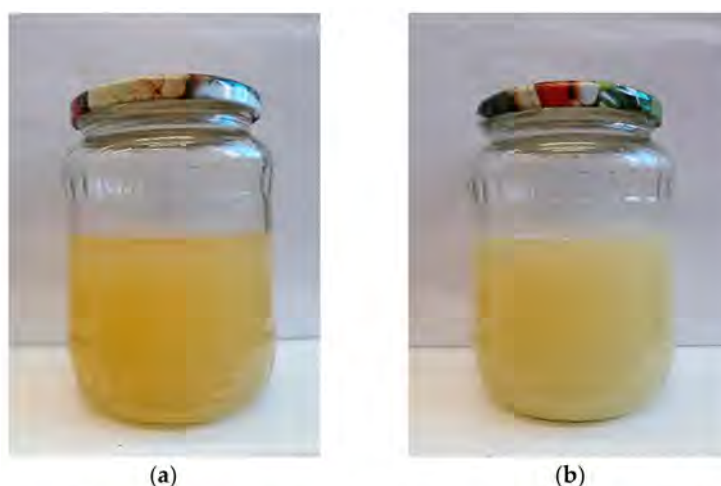

Figure 2. Test fuel blends after application of stirring: (**a**) M10, (**b**) M20.

2.2. Equipment Used

A turbocharged compression ignition engine (Zetor 1204) was used for the measurements and mounted on the tractor (Zetor Forterra 8641). The tractor was not equipped with a diesel particulate filter (DPF). The basic specifications of the test engine are given in Table 2. The test engine complies with Tier II emission limits for nonroad vehicles (Table 3).

A mobile swirl dynamometer (MAHA ZW 500) was used to load the engine via the power-takeoff shaft (PTO). Energy losses in the power transmission do not affect the comparative measurements; therefore, these losses were not considered. The basic parameters of the dynamometer are listed in Table 4. Data from the dynamometer were recorded by its own data acquisition unit, provided by the manufacturer. Ambient conditions, such as atmospheric pressure, temperature, and humidity, were also monitored using built-in sensors in the MAHA data acquisition unit. Exhaust gas temperature was measured in the exhaust manifold by a K-type thermocouple. All data were recorded with a frequency of 10 Hz. The tractor, with the dynamometer connected to it, is shown in Figure 3.

Table 2. Test engine specifications.

Parameter	Specification
Manufacturer and type	Zetor 1204
Cylinders	4, in-line
Air fill	Turbocharged
Rated power	60 kW at 2200 rpm (53.4 kW on PTO) [1]
Maximum torque	351 Nm at 1500 rpm (312 Nm on PTO) [1]
Engine displacement volume	4.156 l
Cylinder bore × stroke	105 × 120 mm
Compression ratio	17
Combustion chamber	Bowl-in-piston
Fuel supply	Mechanical in-line injection pump
Injection type	Direct injection
Start of injection (SOI)	12° BTDC
Injection pressure (injector opening pressure)	22 MPa
Injector nozzle	Multihole
Valve mechanism	OHV
Valves per cylinder	2
Cooling system	Liquid-cooled
PTO gear ratio	3.543

[1] according to Deutsche Landwirtschafts-Gesellschaft.

Table 3. Tier II Emission limits for nonroad engines (results of the standardized nonroad steady cycle according to ISO 8178-4—type C1).

Emission Component	Limit Value (g/kWh)
Carbon monoxide	5
Hydrocarbons	1.3
Nitrogen oxides	7
Particulate matter	0.4

Table 4. Dynamometer specifications.

Parameter	Specifications
Manufacturer and type	Maha ZW 500
Max. power	500 kW
Max. torque	6600 Nm
Max. speed	2500 rpm
Torque inaccuracy	<1% over the full speed range [1]

[1] according to Deutsche Landwirtschafts-Gesellschaft.

Figure 3. Tractor and the dynamometer used for the measurements: (**a**) Zetor Forterra 8641, (**b**) MAHA ZW500.

The Fourier-transform infrared (FTIR) spectroscopy analyzer (Bruker MATRIX-MG5) was used for exhaust emissions measurements. Its specifications are listed in Table 5. To evaluate the individual emission components from the spectra, a software package (OPUS Gas Analysis (GA)) provided by the manufacturer was used. The emissions of carbon dioxide (CO_2), carbon monoxide (CO), nitrogen oxides (NO_X), formaldehyde (HCHO), methane (CH_4), acetaldehyde (CH_3CHO), and butadiene (C_4H_6) were monitored. NO_X represents the sum of emissions of nitric oxide (NO) and nitrogen dioxide (NO_2). Data from the emission analyzer were recorded at a frequency of 5 Hz. The mass emission concentrations were calculated using molar masses of the individual emission components from the measured volumetric emission concentrations.

Table 5. Specifications of FTIR emission analyzer (Bruker Matrix MG5).

Parameter	Specifications
Spectral range	4800–750 cm^{-1}
Detector	Liquid nitrogen cooled Mercury–Cadmium–Telluride
Interferometer	Rocksolid™, permanently aligned
Spectral resolution	<1 cm^{-1}
Spectral rate	4 spectra at 4 cm^{-1} spectral resolution 1 spectrum at 0.5 cm^{-1} spectral resolution
Wavenumber accuracy	>0.05 cm^{-1}
Photometric accuracy	>0.1%

The soot particles were measured and analyzed by an engine exhaust particle sizer (EEPS) spectrometer (TSI 3090). The basic specifications of EEPS are shown in Table 6. Before entering the EEPS, the exhaust gas was diluted (dilution ratio 0.01007, dilution factor 99.2667). The dilution machine and hoses of the exhaust engine particle sizer were heated to 150 °C to prevent the volatile fractions from forming condensate. Data from the EEPS were recorded with a frequency of 1 Hz.

Table 6. Specifications of the EEPS.

Parameter	Specifications
Particle size range	5.6–560 nm
Particle size resolution	16 channels per decade (32 total)
Electrometer channels	22
Charger mode of operation	Unipolar diffusion charger
Inlet cyclone 50% cutpoint	1 μm
Time resolution	10 size distributions s^{-1}

According to Equation (1), fuel consumption was calculated based on the monitored carbon-containing emissions, CO_2, CO, HCHO, CH_3CHO, CH_4, and C_4H_6, air mass flow rate, and carbon content of the test fuels, as listed in Table 1. The mass flow rate of air was measured using a lossless nozzle and U-tube. The mass flow rate of air was calculated based on the pressure difference and the intake air temperature.

$$FC = \left(\sum \frac{C_i}{100} \times E_i \right) \times \frac{100}{C_F} \tag{1}$$

where: FC—fuel consumption (kg/h); E_i—mass production of the individual carbon-containing emission component (CO_2, CO, HCHO, CH_3CHO, CH_4, C_4H_6) (kg/h); C_i—mass concentration of carbon in the individual emission component (%wt); C_F—mass concentration of carbon in the fuel as can be seen in Table 1 (%wt).

2.3. Measurement Methodology

The measurements were performed in stable engine conditions at constant speed at different loads to analyze the effect of test fuels on the engine's performance characteristics.

The engine's speed was maintained at 1950 rpm since, at this speed, the PTO shaft reaches its nominal value, required for the proper function of agricultural equipment. Therefore, it can be assumed that the engine spends most of its operation time at this rotation speed.

The load of the engine was selected as ~50% (point 1), ~70% (point 2), and ~100% (point 3), while the torque was calculated from the maximum torque using D100 at the corresponding speed. The values of torque for individual measurement points and fuels are given in Table 7.

Table 7. Brake torque, calculated for individual measurement points.

Fuel	Calculated Torque at the PTO (Nm)		
	Point 1	Point 2	Point 3
D100	500	700	973
M5	500	700	Full
M10	500	700	Full
M20	500	700	Full

After the required torque was set, the engine was thermally stabilized for ~1–1.5 min. After the stabilization, the data were recorded for ~80s. The scheme of the measurements is given in Figure 4.
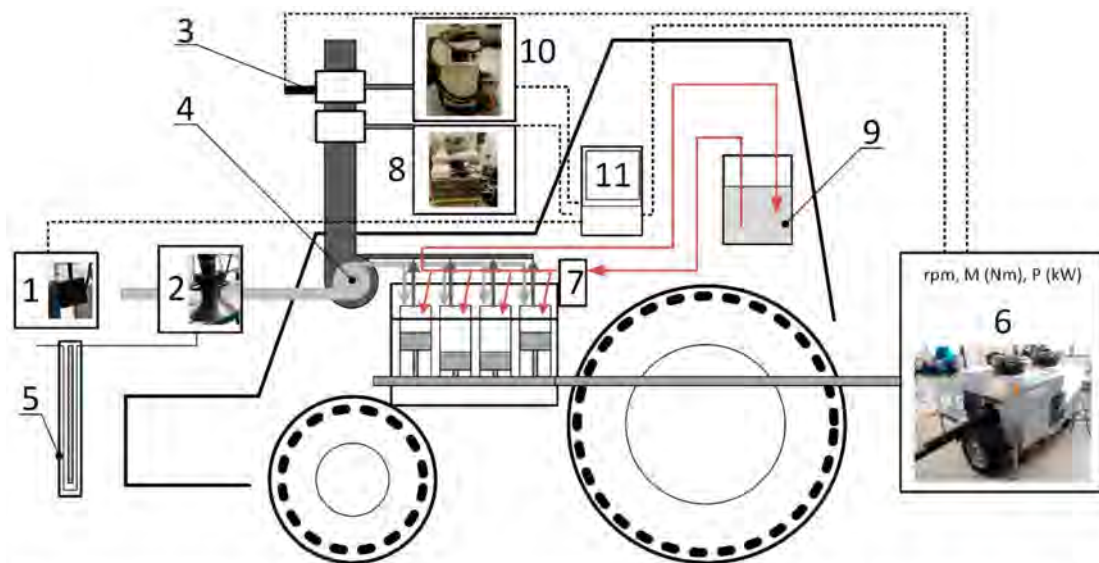

Figure 4. Measurement scheme: 1—sensors for pressure and temperature of the intake air, 2—lossless nozzle, 3—exhaust gas temperature sensor, 4—turbocharger, 5—U-tube manometer, 6—dynamometer, 7—fuel pump, 8—emission analyzer, 9—fuel tank, 10—EEPS, 11—PC for control and data acquisition.

Rotation speed characteristics were measured for each fuel blend before the individual points to determine the effect of test fuels on the engine performance parameters.

The analysis of variance (ANOVA), complemented with Tukey honestly significant difference (HSD) post hoc test, was used to verify gaseous exhaust emissions and soot particle formation results. The set of values of each parameter are given by the individual recording frequency of each measured parameter (emission analyzer—5 Hz, soot particles—1 Hz) and actual recording time (~1–1.5 min).

3. Results and Discussion

3.1. Performance Parameters, Fuel Consumption, Thermal Efficiency

In this subsection, the effect of the blended fuels on the engine torque, power, fuel consumption, and engine efficiency are shown and analyzed. In Figure 5, the external speed characteristics of torque and power can be seen. The figure shows that all of the blended

fuels caused deterioration in engine performance parameters. M5 caused a decrease in maximum power by ~7.1% and torque by ~9.4%; whereas M10 caused a decrease in maximum power by ~11.2% and torque by ~13.4%; and when running on M20, the engine power decreased by ~22.5% and torque by ~27% in comparison to D100. The deterioration in performance parameters was mainly caused by the lower calorific value of the fuel blends. In the case of M20, the worsened efficiency also contributed to the deterioration in the engine performance due to its high alcohol content having a lower cetane number.
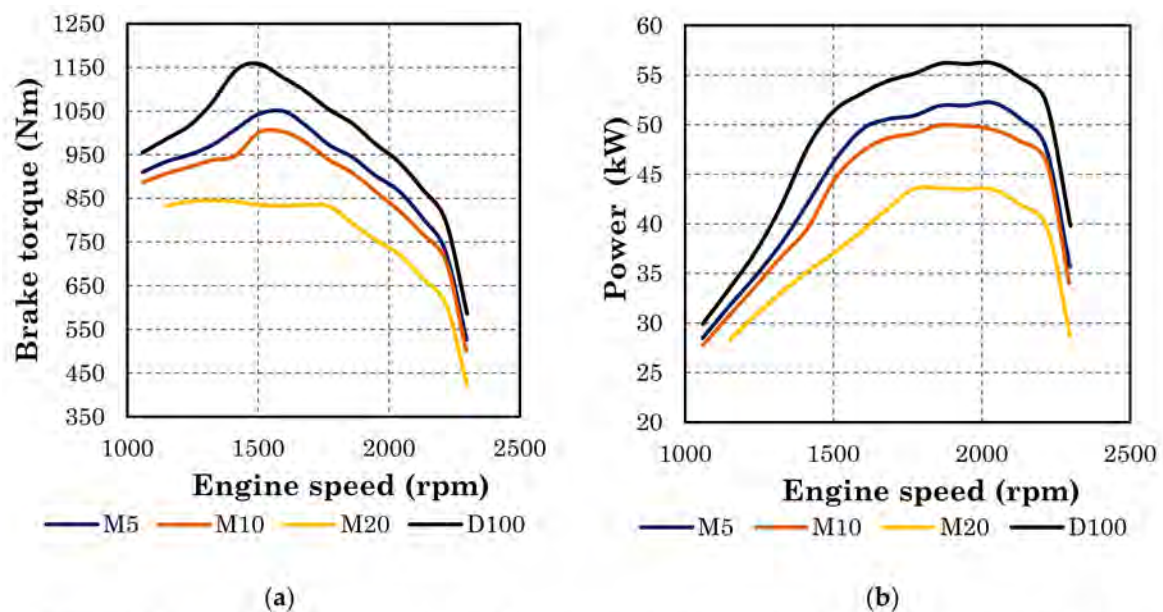
Figure 5. External speed characteristics of the engine: (**a**) brake torque, (**b**) engine power on the PTO.

In Figure 6, the achieved values of the brake torque for individual measurement points are shown. For measurement points 1 and 2, the differences were >3%. For measurement point 3, at full engine load, the lower calorific values of the blended fuels caused a reduction in the brake torque compared to D100 by 6.17%, 9.51%, and 20.14% when using M5, M10, and M20, respectively. Decreased engine performance was also found by other studies dealing with the fuel blends of diesel, vegetable oils, and alcohols [86–88]. Ileri et al. [89] tested diesel–rapeseed oil–butanol blends in the ratio: 70% diesel, 20% rapeseed oil, and 10% butanol, and found decreased average brake torque by ~4–5%. Atmanli [88] found decreasing brake torque with an increasing amount of alcohol fraction in the fuel blend at full engine load in the whole range of engine speed. In contrast, Atmanli et al. [90] tested ternary blends with various vegetable oils and butanol in the volume concentration of 70–20–10 and found increased brake torque at high engine speed by ~1–4%, depending on the vegetable oil used; however, on average, the brake torque decreased by ~1–2%. The decrease of engine performance is explained above all by the low calorific value of alcohol fraction in the fuel blends and its low cetane number [88].
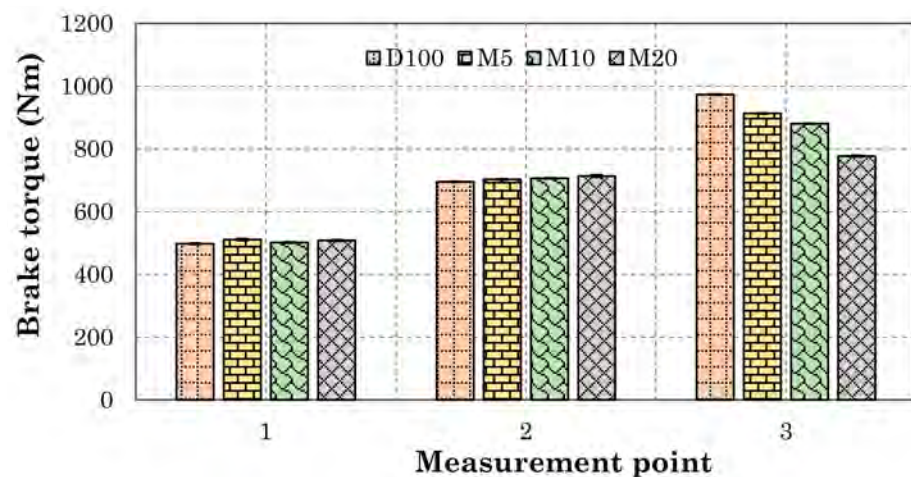
Figure 6. Brake torque for all test fuels at the measurement points (error bars represent the standard deviation).

In Figure 7, the brake-specific fuel consumption (BSFC) for all test fuels at all measurement points is shown. An increase in BSFC was expected due to the lower calorific value of the blended fuels compared with D100. The highest difference compared to D100 using all test fuels was achieved at the measurement point 3. For M5, the BSFC increased by ~9.81%, M10 by ~15.68%, and M20, BSFC increased by ~26.51%.
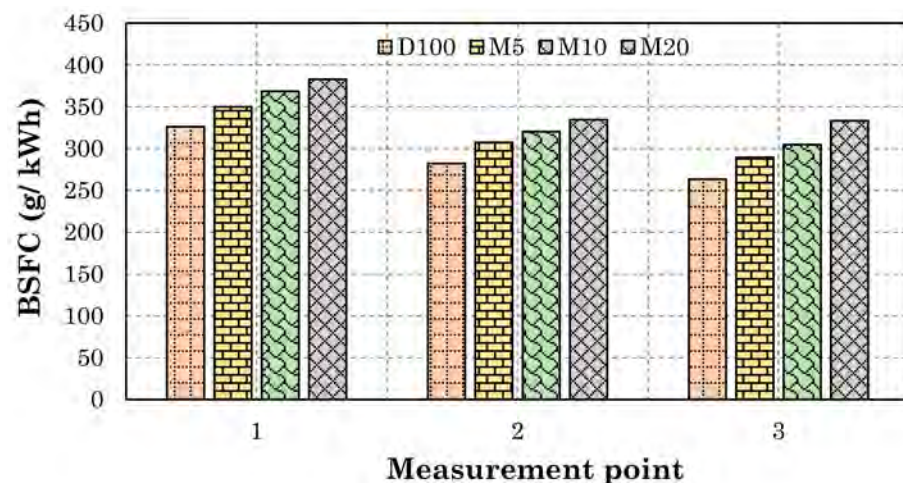

Figure 7. Brake-specific fuel consumption of all test fuels at the measurement points.

The brake thermal efficiency (BTE), reached with all test fuels at all measurement points, is shown in Figure 8. The M5 and M10 reached similar values of BTE as D100 (the differences were >2%). At measurement point 3, M20 caused a decrease in BTE by ~5.26% compared to D100. Increased BSFC and reduced BTE were found in the studies using ternary blends of vegetable oil, diesel, and alcohol [86,88–91] and alcohol–diesel blends [92–95]. However, in most studies, higher differences were found at the lower engine loads. Atmanli et al. [90] found increased BSFC and decreased BTE using ternary blends of various vegetable oils, diesel, and butanol at full engine load. The reduction of BTE was in the range ~13–15%, and the increase of BSFC in the range ~30–80%. Sayin et al. [93] found reduced BTE when using diesel–methanol blends with methanol concentrations of 5%, 10%, and 15%. For 15% methanol, the reduction was ~30%. However, for 10% and lower methanol concentrations, the reductions were ~10% at high engine load. The same study [93] also found increased BSFC with increased methanol in the fuel blends.
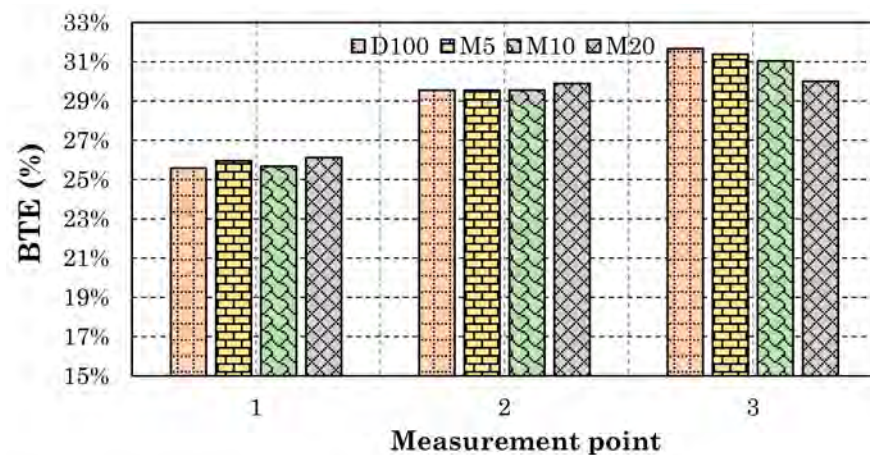
Figure 8. Brake thermal efficiency of all test fuels at the measurement points.

3.2. Gaseous Emissions

In this section, the effect of the blended fuels on specific emissions of CO_2, CO, NO_X, HCHO, C_4H_6, and CH_4 and the production of soot particles is presented. The measured emissions of CH_3CHO were below the instrumental measurement accuracy for all test fuels, and the differences were inconclusive. Figure 9 shows the specific emissions of CO_2 using all test fuels at all measurement points. It is evident that at measurement points 1 and 2, the differences between the blended fuels and D100 are negligible (>2%). At full load (point 3), all blended fuels caused an increase in the specific emissions of CO_2 compared to D100 (M5—2.03%, M10—3.49%, M20—5.47%). This increase in specific emissions of CO_2 is due to the combed effect of lower BTE at full load and lower calorific value of the test fuels, leading to lower power output. ANOVA, complemented with the Tukey HSD post hoc test, showed a statistically significant difference between all test fuels at all measurement points. The example of ANOVA results for CO_2 at point 2 is shown in Table 8.
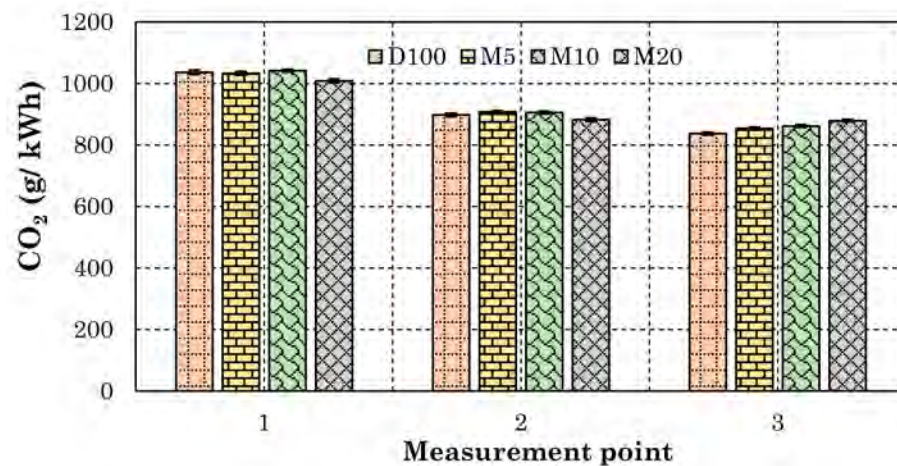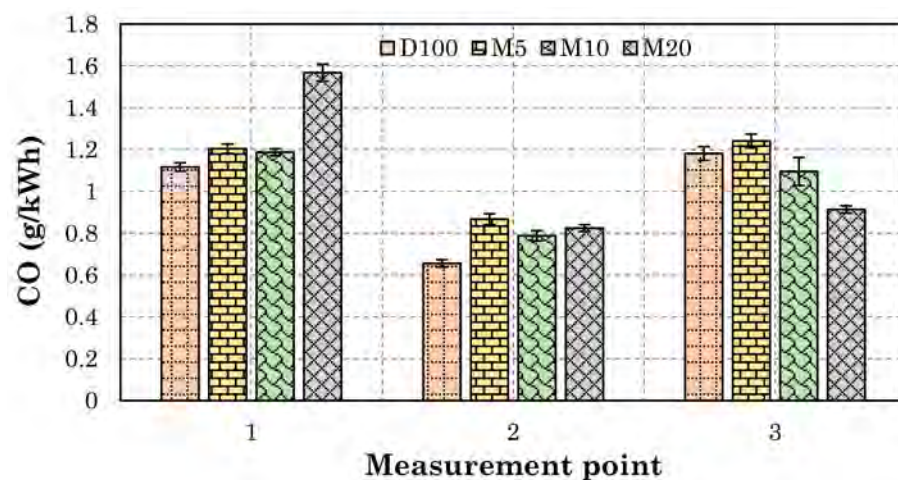

Figure 9. Specific emissions of CO_2 for all test fuels at all measurement points (error bars represent the standard deviation).

Table 8. Results of ANOVA with Tukey HSD post hoc test for CO_2 at the measurement point 2.

		ANOVA		
α = 0.05	Sum of Squares	Degrees of Freedom	Variance	F
Between groups	88,304.56	3	29,434.85	1041.8031
Within groups	31,672.46	1121	28.2538	
Total	119,977.02	1124		
		Tukey HSD post hoc test		
D100 vs. M5: Diff = 9.6392, 95% CI = 8.5337 to 10.7446, *p* = 0.0000				
D100 vs. M10: Diff = 7.8299, 95% CI = 6.7532 to 8.9067, *p* = 0.0000				
D100 vs. M20: Diff = −15.3853, 95% CI = −16.6075 to −14.1631, *p* = 0.0000				
M5 vs. M10: Diff = −1.8092, 95% CI = −2.9372 to −0.6813, *p* = 0.0002				
M5 vs. M20: Diff = −25.0245, 95% CI = −26.2920 to −23.7569, *p* = 0.0000				
M10 vs. M20: Diff = −23.2152, 95% CI = −24.4578 to −21.9727, *p* = 0.0000				

Specific emissions of CO for all test fuels at all measurement points are shown in Figure 10. It can be seen that at measurement points 1 and 2, the specific emissions of CO increased when using all test fuels compared to D100. The highest difference was achieved using the M20 at the measurement point 1 (~41.9%). At measurement point 3, increasing the alcohol concentration in the test blend decreased the specific emission of CO. This reduction may be caused by an increased oxygen content in the fuel blends, which is also evident from the emission of CO_2. A statistically significant difference in specific emissions of CO was found between all test fuels at all measurement points. The example of ANOVA results for CO at the measurement point 2 is shown in Table 9.

Figure 10. Specific emissions of CO for all test fuels at all measurement points (error bars represent the standard deviation).

An increase in CO emission compared with diesel was found mainly in the studies using vegetable oil–diesel–alcohol ternary blends [41,86,88–90,96]. Lujaji et al. [96] reported increased concentration of CO in the exhaust gas of a 1.9 L turbocharged CI engine using blends of diesel, croton oil, and butanol at 25–75% engine load. The highest difference was detected at 20% engine load. At 100% engine load, the concentration of CO emission decreased. Atmanli et al. [86] found increased specific emissions of CO using blends of diesel, butanol, and different vegetable oils at full load at seven out of eight measured points. The highest difference was found at the lowest engine speed. When using the alcohol–diesel blends, CO emission was usually lower. However, Zhang et al. [92] found increased CO emission when using methanol fumigation in a four-cylinder diesel engine.

Table 9. Results of ANOVA with Tukey HSD post hoc test for CO at the measurement point 2.

ANOVA				
$\alpha = 0.05$	Sum of Squares	Degrees of Freedom	Variance	F
Between groups	7.7138	3	2.5713	5482.1678
Within groups	0.5258	1121	0.0005	
Total	8.2396	1124		
Tukey HSD post hoc test				
D100 vs. M5: Diff = 0.2114, 95% CI = 0.2069 to 0.2159, p = 0.0000				
D100 vs. M10: Diff = 0.1327, 95% CI = 0.1283 to 0.1370, p = 0.0000				
D100 vs. M20: Diff = 0.1688, 95% CI = 0.1639 to 0.1738, p = 0.0000				
M5 vs. M10: Diff = −0.0787, 95% CI = −0.0833 to −0.0741, p = 0.0000				
M5 vs. M20: Diff = −0.0426, 95% CI = −0.0477 to −0.0374, p = 0.0000				
M10 vs. M20: Diff = 0.0362, 95% CI = 0.0311 to 0.0412, p = 0.0000				

Brake-specific NO_X emissions for all test fuels at all measurement points are given in Figure 11. NO_X emissions depend strongly on the peak in-cylinder temperature in the premixed combustion stage and the amount of free oxygen available locally [64]. NO_X formation requires sufficient reaction time for oxidation reactions to proceed [62]. The fuel blends exhibited higher specific NOx emissions at all measurement points. An increase in NO_X emissions was mainly due to the higher oxygen content of the blends and higher combustion rate of evaporated lighter fractions, giving higher temperature gradients. The higher vegetable oil content also contributes to higher NO_X emissions [90], especially at measurement points 2 and 3, as seen in Figure 11. The increase was most significant at the measurement point 1, at ~50% engine load. This may be connected with a higher amount of free oxygen since a lower amount of fuel is injected into the cylinder, and thus higher air-fuel ratio is achieved. The effect of oxygen in NO_X emissions is also demonstrated in Figure 12, where a breakup of the NO_X constituents (NO and NO_2) can be seen. It is evident that with increasing oxygen content in the fuel blends, the proportion of NO_2 also increases.
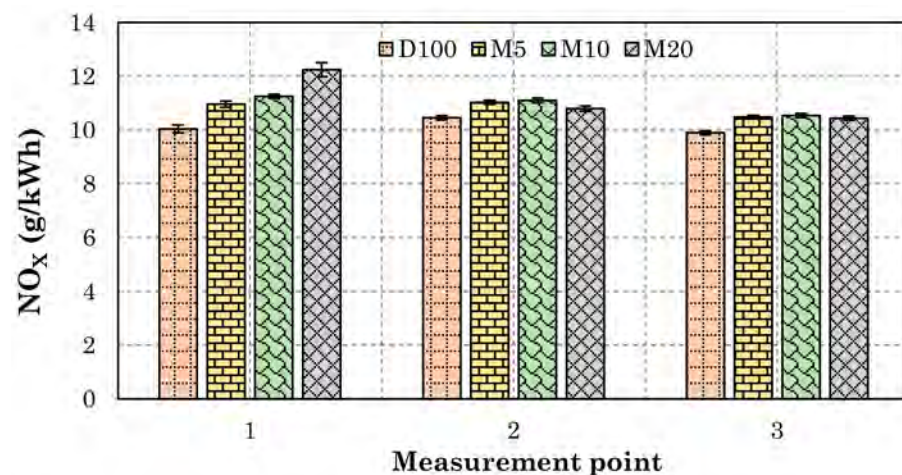
Figure 11. Specific NO_X emissions for all test fuels at all measurement points (error bars represent the standard deviation).
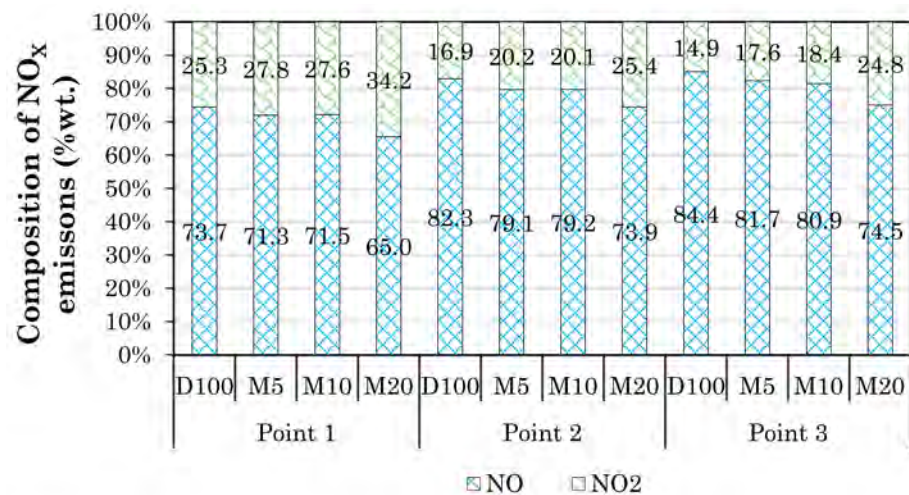
Figure 12. Constituents of NO_X emissions for all test fuels at all measurement points.

When using M5, the increase of specific emissions of NO_X was 9.16%, 5.49%, and 5.88%; for M10, this increase was 12.09%, 6.13%, and 6.44%; and for M20, this increase was 21.92%, 3.26%, and 5.46% at measurement points 1, 2, and 3, respectively. The differences between all test fuels at all measurement points were statistically significant. The results of ANOVA for specific NO_X emissions at the measurement point 3 with the Tukey HSD post hoc test is shown in Table 10. Slightly lower specific NO_X emissions were achieved with M20 at measurement points 2 and 3. This may be due to lower combustion temperatures than other test fuels, caused by evaporation of alcohols in the blends having a relatively higher latent heat of vaporization, combined with a lower amount of free oxygen than measurement point 1.

Table 10. Results of ANOVA with Tukey HSD post hoc test for NO_X at the measurement point 3.

ANOVA				
$\alpha = 0.05$	Sum of Squares	Degrees of Freedom	Variance	F
Between groups	82.6574	3	27.5525	5240.5733
Within groups	6.1776	1175	0.0053	
Total	88.8350	1178		
Tukey HSD post hoc test				
D100 vs. M5: Diff = 0.5827, 95% CI = 0.5678 to 0.5977, $p = 0.0000$				
D100 vs. M10: Diff = 0.6374, 95% CI = 0.6228 to 0.6520, $p = 0.0000$				
D100 vs. M20: Diff = 0.5408, 95% CI = 0.5244 to 0.5571, $p = 0.0000$				
M5 vs. M10: Diff = 0.0547, 95% CI = 0.0399 to 0.0694, $p = 0.0000$				
M5 vs. M20: Diff = -0.0420, 95% CI = -0.0584 to -0.0255, $p = 0.0000$				
M10 vs. M20: Diff = -0.0967, 95% CI = -0.1128 to -0.0805, $p = 0.0000$				

The exhaust gas temperature is shown in Figure 13. Increased NO_X emissions, including lower exhaust gas temperature, were found in other studies using diesel–methanol blends [62,64,94], and vegetable oil–diesel–butanol blends [41,86–90]. Jamrozik et al. [64] found increased specific NO_X emissions when testing diesel–methanol blends up to 40% of methanol in a naturally aspirated single cylinder CI engine by up to 127%. At the same time, the EGT decreased by up to ~16%. Atmanli et al. [86] found increased NO_X emissions while running a 2.5 L turbocharged CI engine at full load at various engine speeds using ternary blends of vegetable oil, diesel, and butanol. The average increase was ~30%, while the EGT decreased on an average by ~15%. Other studies [93,95,97] also reported increased NO_X emission from diesel blended with alcohols, including methanol

and butanol. However, in these studies, an increased combustion temperature was also reported.
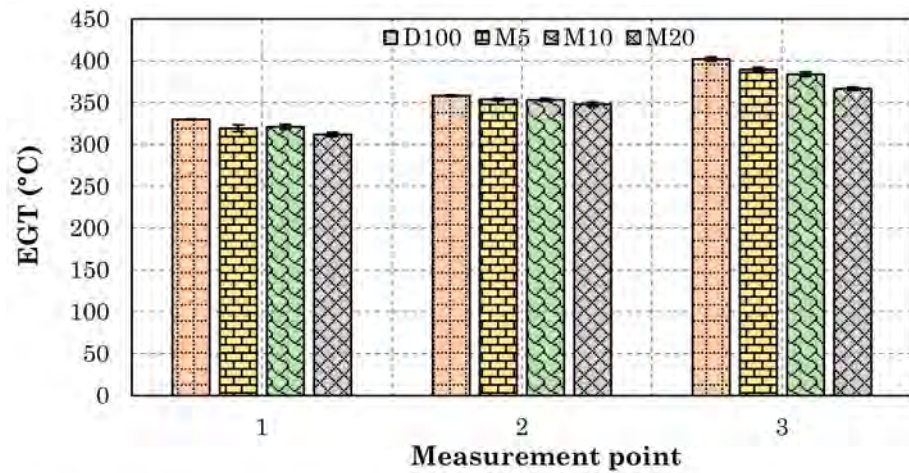

Figure 13. Exhaust gas temperature (EGT) for all test fuels at all measurement points (error bars represent the standard deviation).

Figure 14 shows the HCHO emissions for all test fuels at all measurement points. HCHO is listed as carcinogenic to humans (highest risk) by International Agency for Research on Cancer (IARC) [98]. Emissions of HCHO are usually associated with the combustion of methanol since HCHO is an intermediate product in methanol oxidation reactions [50,53,92]. All of the test fuel blends caused an increase in specific HCHO emissions. Compared to D100, M5 caused an increase by 46.18%, 77.79%, 30.99%; M10 by 42.37%, 63.84%, 23.22%; and M20 by 61.38%, 100.7% and 15.76% at measurement points 1, 2, and 3, respectively. All of the differences between the test fuels within individual measurement points were found to be statistically significant. The results of ANOVA for specific emissions of HCHO at the measurement point 3 complemented with the Tukey HSD post hoc test is shown in Table 11. Increased specific emissions of HCHO were found mainly in the studies using methanol–diesel blends [92,99,100]. Wei et al. [100] found increased emissions of HCHO up to 65.5 times, using methanol–diesel blends in concentrations up to 70% of methanol.
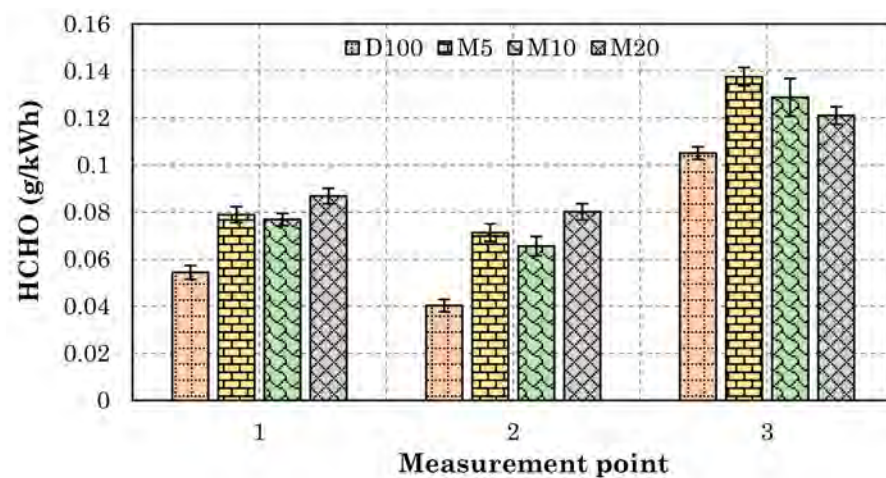

Figure 14. Specific HCHO emissions for all test fuels at all measurement points (error bars represent the standard deviation).

Table 11. Results of ANOVA with Tukey HSD post hoc test for HCHO at the measurement point 3.

ANOVA				
$\alpha = 0.05$	Sum of Squares	Degrees of Freedom	Variance	F
Between groups	0.1785	3	0.0595	2223.3071
Within groups	0.0315	1175	0.0000	
Total	0.2100	1178		
Tukey HSD post hoc test				
D100 vs. M5: Diff = 0.0325, 95% CI = 0.0314 to 0.0336, $p = 0.0000$				
D100 vs. M10: Diff = 0.0237, 95% CI = 0.0227 to 0.0247, $p = 0.0000$				
D100 vs. M20: Diff = 0.0160, 95% CI = 0.0148 to 0.0172, $p = 0.0000$				
M5 vs. M10: Diff = -0.0088, 95% CI = -0.0098 to -0.0077, $p = 0.0000$				
M5 vs. M20: Diff = -0.0165, 95% CI = -0.0177 to -0.0153, $p = 0.0000$				
M10 vs. M20: Diff = -0.0077, 95% CI = -0.0088 to -0.0065, $p = 0.0000$				

Specific butadiene (C_4H_6) emissions for all test fuels at all measurement points are shown in Figure 15. Butadiene is listed as a probable carcinogen to humans by IARC [98]. The increasing alcohol fraction in the blends tends to increase the specific emissions of butadiene compared to D100. For M5, the increase was 15.09%, 17.18%, and 26.03%; for M10, the increase was 28.74%, 26.29%, and 37.31%; and for M20, the increase was 54.23%, 54.3%, and 82.5% at measurement points 1, 2, and 3, respectively. All of the measured differences within the individual measurement points were found statistically significant. Table 12 shows the results of ANOVA with the Tukey HSD post hoc test for specific emissions of butadiene. As a hydrocarbon, butadiene is formed due to prematurely terminated oxidation reactions. Therefore, its increase may be connected with the longer ignition delay due to the lower cetane number of methanol and iso-butanol in the fuel blends. In addition, the evaporation of alcohols with the higher latent heat of vaporization decreases the local temperature so that the mixture remains partially unburned [62]. It is also evident that specific emissions of C_4H_6 decrease with increasing engine load, which offer higher combustion temperature and superior oxidation conditions.
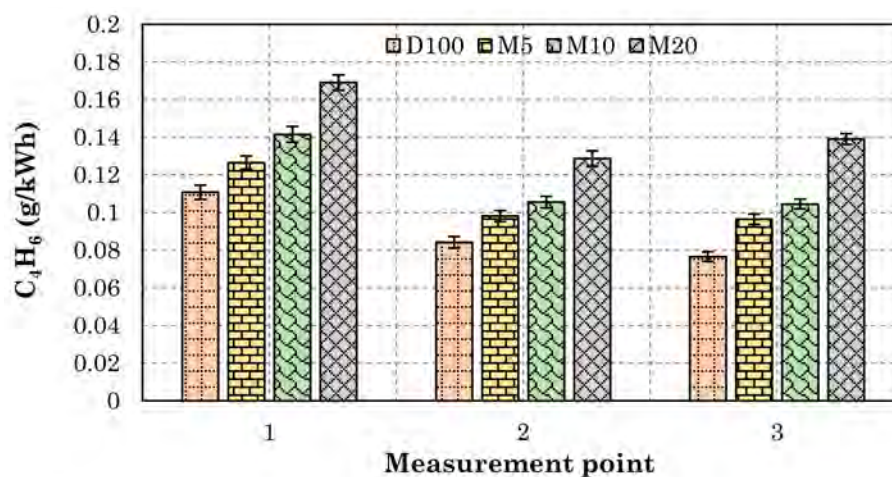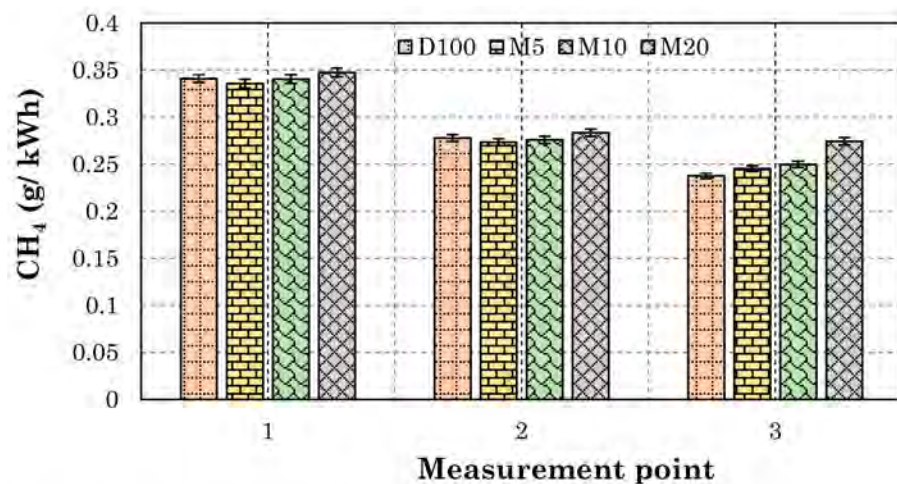

Figure 15. Specific butadiene emissions for all test fuels at all measurement points (error bars represent the standard deviation).

Table 12. Results of ANOVA with Tukey HSD post hoc test for C_4H_6 at the measurement point 2.

ANOVA				
$\alpha = 0.05$	Sum of Squares	Degrees of Freedom	Variance	F
Between groups	0.2562	3	0.0854	8113.0261
Within groups	0.0118	1121	0.0000	
Total	0.2680	1124		
Tukey HSD post hoc test				
D100 vs. M5: Diff = 0.0140, 95% CI = 0.0133 to 0.0146, *p* = 0.0000				
D100 vs. M10: Diff = 0.0214, 95% CI = 0.0207 to 0.0220, *p* = 0.0000				
D100 vs. M20: Diff = 0.0445, 95% CI = 0.0437 to 0.0452, *p* = 0.0000				
M5 vs. M10: Diff = 0.0074, 95% CI = 0.0067 to 0.0081, *p* = 0.0000				
M5 vs. M20: Diff = 0.0305, 95% CI = 0.0298 to 0.0313, *p* = 0.0000				
M10 vs. M20: Diff = 0.0231, 95% CI = 0.0224 to 0.0239, *p* = 0.0000				

Specific emissions of methane (CH_4) for all test fuels at all measurement points are shown in Figure 16. Similar to the butadiene emissions, the specific emissions of CH_4 tend to increase with an increasing proportion of alcohols in the blends compared to D100, especially at full load conditions. However, in the case of methane, the differences are smaller than in the case of butadiene. For measurement points 1 and 2, the differences between all test fuels were >3%. At measurement point 3, the fuel blends M5, M10, and M20 increase specific methane emissions by 3.3%, 5.73%, and 15.97%, respectively, compared to D100. Except for the difference between D100 and M10, which was statistically insignificant (as seen in Table 13), all measured differences between the test fuels were statistically significant.

Figure 16. Specific methane emissions for all test fuels at all measurement points (error bars represent the standard deviation).

Increased emissions of hydrocarbons were observed in the studies exploring diesel–methanol blends [64,100] and vegetable oil–diesel–alcohol ternary blends [87,91,96]. Wei et al. [100] used high premixed ratios of methanol in diesel (up to 70%) to power a six-cylinder turbocharged CI engine. They found an increase of unburned hydrocarbon emissions up to 55.7 times. Sharon et al. [91] found increased emissions of hydrocarbons compared to diesel when fueling a stationary, constant-speed CI engine with blends of diesel, used palm oil, and butanol. At 100% engine load, the increase was ~32%.

Table 13. Results of ANOVA with Tukey HSD post hoc test for CH$_4$ at the measurement point 1.

ANOVA				
α = 0.05	Sum of Squares	Degrees of Freedom	Variance	F
Between groups	0.0201	3	0.0067	331.9628
Within groups	0.0241	1198	0.0000	
Total	0.0442	1201		
Tukey HSD post hoc test				
D100 vs. M5: Diff = −0.0054, 95% CI = −0.0063 to −0.0045, *p* = 0.0000				
D100 vs. M10: Diff = −0.0005, 95% CI = −0.0014 to 0.0004, *p* = 0.5125				
D100 vs. M20: Diff = 0.0065, 95% CI = 0.0055 to 0.0075, *p* = 0.0000				
M5 vs. M10: Diff = 0.0049, 95% CI = 0.0039 to 0.0058, *p* = 0.0000				
M5 vs. M20: Diff = 0.0119, 95% CI = 0.0109 to 0.0128, *p* = 0.0000				
M10 vs. M20: Diff = 0.0070, 95% CI = 0.0060 to 0.0080, *p* = 0.0000				

3.3. Soot Particles

Figure 17 shows the total mass of the soot particles in size range of 5.6–560 nm. It can be seen that the total mass of the soot particles decreased with an increasing proportion of alcohols in the fuel blends compared to D100. The highest reduction was achieved with all test fuel blends at full engine load at the measurement point 3 (M5—47.65%, M10—57.32%, and M20—80.62%). The measured differences between the test fuels were statistically significant. ANOVA results with the Tukey HSD post hoc test for a total mass of soot particles are given in Table 14. The reduction in soot particle production can be explained mainly by an increased amount of oxygen in the fuel blends and a higher proportion of light fractions in the higher volatility and faster oxidation process. Moreover, the lower viscosity of M20 also contributed to reduced particulate mass.
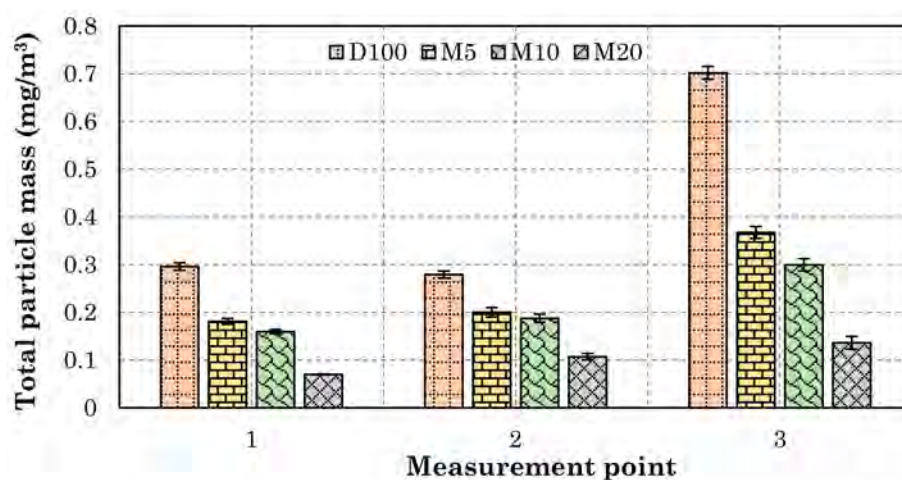

Figure 17. The total mass of soot particles in size range 5.6–560 nm for all test fuels at all measurement points (error bars represent the standard deviation).

Table 14. Results of ANOVA with Tukey HSD post hoc test for soot particles generation at the measurement point 2.

ANOVA				
$\alpha = 0.05$	**Sum of Squares**	**Degrees of Freedom**	**Variance**	**F**
Between groups	1.0623	3	0.3541	5171.0292
Within groups	0.0197	288	0.0001	
Total	1.0820	291		
Tukey HSD post hoc test				
D100 vs. M5: Diff = −0.0790, 95% CI = −0.0824 to −0.0755, $p = 0.0000$				
D100 vs. M10: Diff = −0.0916, 95% CI = −0.0949 to −0.0883, $p = 0.0000$				
D100 vs. M20: Diff = −0.1722, 95% CI = −0.1758 to −0.1685, $p = 0.0000$				
M5 vs. M10: Diff = −0.0126, 95% CI = −0.0162 to −0.0091, $p = 0.0000$				
M5 vs. M20: Diff = −0.0932, 95% CI = −0.0970 to −0.0894, $p = 0.0000$				
M10 vs. M20: Diff = −0.0806, 95% CI = −0.0843 to −0.0768, $p = 0.0000$				

The mean size of the particles, calculated as a weighted average for all test fuels at all measurement points, is shown in Figure 18. All blended fuels caused a significant reduction in the mean particle size, especially at measurement points 1 and 2. The maximum difference achieved using all fuel blends at the measurement point 2 was ~70.78%, 72.12%, and 75.43% for M5, M10, and M20, respectively. This may be caused by the evaporation of the alcohol fraction of the fuel blends. Lower soot particle generation and reduced mean particle size were also achieved by methanol–diesel–dodecanol blends, butanol–diesel blends [101], vegetable oil–diesel–n-butanol blends [5], biodiesel–n-butanol blends [102], and diesel–biodiesel–butanol blends [103]. Zhang et al. [103] found a decreased mass of soot generated after adding butanol in the diesel–biodiesel blend by up to 25%. Another study [104] found decreased production of ultrafine soot particles up to ~60% when using 10% and 15% methanol blended in diesel with a 1% dodecanol.
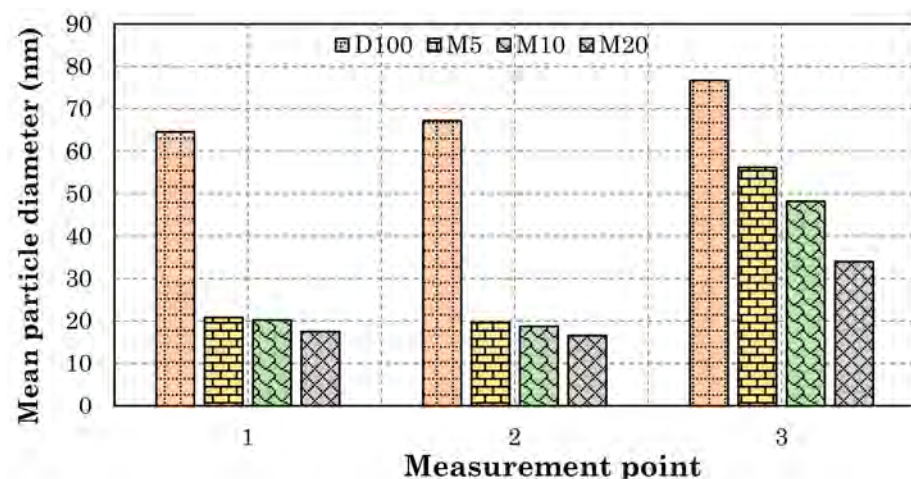

Figure 18. Mean diameter of soot particles in size range 5.6–560 nm for all test fuels at all measurement points.

Figure 19 shows the size distribution of soot particles for all test fuels at the measurement point 3. The increasing alcohol content caused tiny particles in size range ~7–14 nm. This may be due to the evaporation of the light fractions during the ignition delay. In addition, the high deviations of the particle count in the size range ~8–12 nm may be connected with the relatively unstable engine operation compared to D100, especially when using M20. Similar results of the soot particle size distribution were reported for vegetable oil–diesel–butanol blends [5], biodiesel–butanol blends [102], biodiesel–diesel–butanol blends [103], and diesel–vegetable oil blends [18].
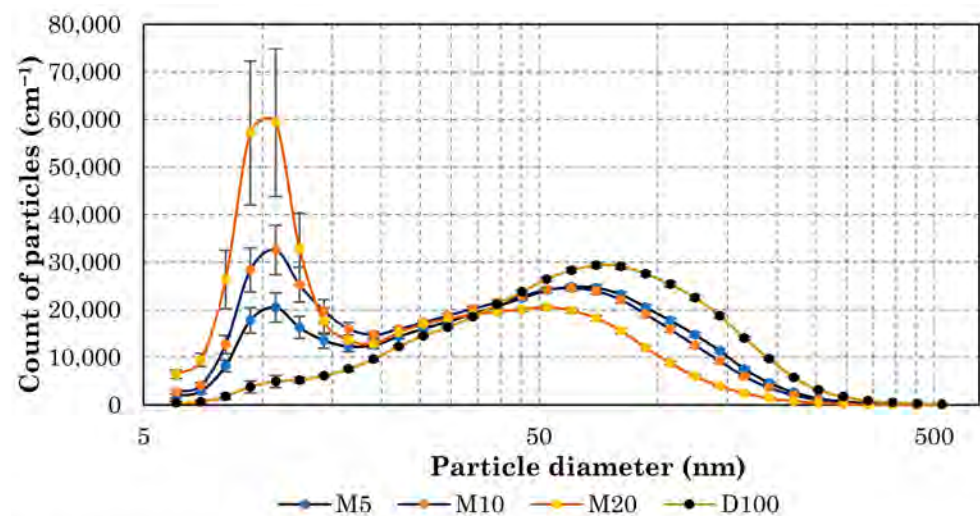
Figure 19. Size distribution of the soot particles in size range 5.6–560 nm at measurement point 3 for all test fuels (error bars represent the standard deviation).

4. Conclusions

From the experimental results focused on exploring the effect of diesel–vegetable oil–methanol–iso-butanol blends on the engine performance, efficiency, emissions, and soot particles, the following conclusions could be made:

- With an increasing proportion of alcohols in the blend, the performance parameters deteriorated due to the lower calorific value of the blended fuels. Maximum brake torque decreased by up to 27% and maximum brake power by 22.5% for M20 compared to D100.
- The fuel blends reduced BTE with increasing alcohol content in the blend at full engine load compared to D100 by up to ~5.3%. With the decreased BTE, the specific emissions of CO_2 increased by up to ~5.5%.
- Compared to D100, the specific NO_X emissions increased with increasing oxygen content in the fuel blends, especially at the measurement point 1. In addition, the amount of NO_2 in the NO_X was higher for M20. M20 exhibited a slight reduction in NOx emissions at higher engine loads compared with M5 and M10, which may be caused by the higher latent heat of vaporization of alcohols in the blends.
- Specific emissions of HCHO increased for all test fuel blends compared to D100 since the HCHO is an intermediate product of methanol oxidation. The highest increase was 100.7% for M20 at the measurement point 2.
- The other hydrocarbons evaluated (C_4H_6 and CH_4) increased with increasing alcohol fraction in the fuel blends, which may be caused by locally reduced temperature due to evaporation of alcohols and lower cetane number, causing longer ignition delay.
- With increasing oxygen content in the fuel blends, the mass of soot particles in the size range 5.6–560 nm decreased by up to ~80.6% at full load. However, with a reduction in the mass of soot particles, their mean diameter also decreased by up to ~75% at the measurement point 2. An increasing alcohol fraction promoted the formation of tiny particles.

From the viewpoint of the engine operational parameters tested in this study, the fuel blends containing 5% and 10% methanol seemed to be a suitable compromise. With M20, the adverse effects of deteriorated engine performance and reduced BTE increased BSFC; higher CO, HC, and NO_X emissions were very strong compared to M5 and M10.

This study focused on short-term biofuel applications; the long-term operation remains questionable and requires further research. However, from the general experiences of the researchers and the results of their previous studies focused on long-term utilization of ternary blends of diesel, vegetable oil, and alcohols [105,106], it can be assumed that the

alcohol content may cause a reduction in the engine oil viscosity and accelerate its degradation. Alcohol can also damage the sealing elements due to their general aggressiveness toward rubber and plastics. In addition, their worsened lubricity could mean an increased wear of functional surfaces of the injection system. Furthermore, the vegetable oil content in the blend may lead to carbonaceous deposits in the combustion chamber due to its poor evaporation characteristics and relatively longer hydrocarbon chains in their molecular structures.

References

1. Wang, M.; Wu, M.; Huo, H. Life-cycle energy and greenhouse gas emission impacts of different corn ethanol plant types. *Environ. Res. Lett.* **2007**, *2*, 024001. [CrossRef]
2. Prasad, S.; Kumar, S.; Yadav, K.K.; Choudhry, J.; Kamyab, H.; Bach, Q.-V.; Sheetal, K.R.; Kannojiya, S.; Gupta, N. Screening and evaluation of cellulytic fungal strains for saccharification and bioethanol production from rice residue. *Energy* **2020**, *190*, 116422. [CrossRef]
3. Prasad, S.; Singh, A.; Korres, N.E.; Rathore, D.; Sevda, S.; Pant, D. Sustainable utilization of crop residues for energy generation: A life cycle assessment (LCA) perspective. *Bioresour. Technol.* **2020**, *303*, 122964. [CrossRef]
4. Valera, H.; Agarwal, A.K. Methanol as an Alternative Fuel for Diesel Engines. In *Methanol and the Alternate Fuel Economy*; Springer: Singapore, 2019; pp. 9–33.
5. Čedík, J.; Pexa, M.; Peterka, B.; Müller, M.; Holubek, M.; Hloch, S.; Kučera, M. Combustion characteristics of compression ignition engine fuelled with rapeseed oil–diesel fuel–n-butanol blends. *Oil Gas Sci. Technol.* **2021**, *76*, 17. [CrossRef]
6. Chen, X.; Shuai, C.; Zhang, Y.; Wu, Y. Decomposition of energy consumption and its decoupling with economic growth in the global agricultural industry. *Environ. Impact Assess. Rev.* **2020**, *81*, 106364. [CrossRef]
7. Agarwal, A.K. Biofuels (alcohols and biodiesel) applications as fuels for internal combustion engines. *Prog. Energy Combust. Sci.* **2007**, *33*, 233–271. [CrossRef]
8. Patel, C.; Chandra, K.; Hwang, J.; Agarwal, R.A.; Gupta, N.; Bae, C.; Gupta, T.; Agarwal, A.K. Comparative compression ignition engine performance, combustion, and emission characteristics, and trace metals in particulates from Waste cooking oil, Jatropha and Karanja oil derived biodiesels. *Fuel* **2019**, *236*, 1366–1376. [CrossRef]
9. Dhar, A.; Agarwal, A.K. Effect of Karanja biodiesel blend on engine wear in a diesel engine. *Fuel* **2014**, *134*, 81–89. [CrossRef]
10. Labecki, L.; Cairns, A.; Xia, J.; Megaritis, A.; Zhao, H.; Ganippa, L.C. Combustion and emission of rapeseed oil blends in diesel engine. *Appl. Energy* **2012**, *95*, 139–146. [CrossRef]
11. Rakopoulos, C.D.; Antonopoulos, K.A.; Rakopoulos, D.C.; Hountalas, D.T.; Giakoumis, E.G. Comparative performance and emissions study of a direct injection Diesel engine using blends of Diesel fuel with vegetable oils or bio-diesels of various origins. *Energy Convers. Manag.* **2006**, *47*, 3272–3287. [CrossRef]
12. Haldar, S.K.; Ghosh, B.B.; Nag, A. Studies on the comparison of performance and emission characteristics of a diesel engine using three degummed non-edible vegetable oils. *Biomass Bioenergy* **2009**, *33*, 1013–1018. [CrossRef]
13. Purushothaman, K.; Nagarajan, G. Performance, emission and combustion characteristics of a compression ignition engine operating on neat orange oil. *Renew. Energy* **2009**, *34*, 242–245. [CrossRef]
14. Reksowardojo, I.K.; Brodjonegoro, T.P.; Arismunandar, W.; Sopheak, R.; Ogawa, H. *The Combustion and Exhaust Gas Emission of a Direct Injection Compression Ignition Engine Using Physic Nut Oil (Jatropha Curcas L. Oil)*; SAE Technical Papers; SAE International: Warrendale, PA, USA, 2007.

15. Kalam, M.A.; Masjuki, H.H. Emissions and deposit characteristics of a small diesel engine when operated on preheated crude palm oil. *Biomass Bioenergy* **2004**, *27*, 289–297. [CrossRef]

16. Altun, Ş.; Bulut, H.; Öner, C. The comparison of engine performance and exhaust emission characteristics of sesame oil-diesel fuel mixture with diesel fuel in a direct injection diesel engine. *Renew. Energy* **2008**, *33*, 1791–1795. [CrossRef]

17. Czerwinski, J.; Zimmerli, Y.; Meyer, M.; Kasper, M. A modern HD-diesel engine with rapeseed oil, DPF and SCR. *SAE Tech. Pap.* **2008**, *2008*, 776–790. [CrossRef]

18. Čedík, J.; Pexa, M.; Holůbek, M.; Mader, D.; Pražan, R. Effect of sunflower and rapeseed oil on production of solid particles and performance of diesel engine. *Agron. Res.* **2018**, *16*, 985–996. [CrossRef]

19. Čedík, J.; Pexa, M.; Mader, D.; Pražan, R. Combustion characteristics of compression ignition engine operating on rapeseed oil-diesel fuel blends. *Agron. Res.* **2019**, *17*, 957–973. [CrossRef]

20. Dabi, M.; Saha, U.K. Application potential of vegetable oils as alternative to diesel fuels in compression ignition engines: A review. *J. Energy Inst.* **2019**, *92*, 1710–1726. [CrossRef]

21. Mat, S.C.; Idroas, M.Y.; Hamid, M.F.; Zainal, Z.A. Performance and emissions of straight vegetable oils and its blends as a fuel in diesel engine: A review. *Renew. Sustain. Energy Rev.* **2018**, *82*, 808–823. [CrossRef]

22. Hemmerlein, N.; Korte, V.; Richter, H.; Schröder, G. Performance, exhaust emissions and durability of modern diesel engines running on Rapeseed Oil. *SAE Trans.* **1991**, *100*, 400–415. [CrossRef]

23. Sagan, A.; Blicharz-Kania, A.; Szmigielski, M.; Andrejko, D.; Sobczak, P.; Zawiślak, K.; Starek, A. Assessment of the properties of rapeseed oil enriched with oils characterized by high content of α-linolenic acid. *Sustainability* **2019**, *11*, 5638. [CrossRef]

24. Chew, S.C. *Cold Pressed Rapeseed (Brassica napus) Oil*; Elsevier: Amsterdam, The Netherlands, 2020; ISBN 9780128181881.

25. Laoretani, D.; Fernández, M.; Crapiste, G.; Nolasco, S. Effect of drying operating conditions on canola oil tocopherol content. *Antioxidants* **2014**, *3*, 190–199. [CrossRef] [PubMed]

26. McDonnell, K.P.; Ward, S.M.; McNulty, P.B.; Howard-Hildige, R. Results of Engine and Vehicle Testing of Semirefined Rapeseed Oil. *Trans. ASAE* **2000**, *43*, 1309–1316. [CrossRef]

27. Cvengroš, J.; Považanec, F. Production and treatment of rapeseed oil methyl esters as alternative fuels for diesel engines. *Bioresour. Technol.* **1996**, *55*, 145–150. [CrossRef]

28. Murayama, T.; Oh, Y.T.; Miyamoto, N.; Chikahisa, T.; Takagi, N.; Itow, K. *Low Carbon Flower Buildup, Low Smoke, and Efficient Diesel Operation with Vegetable Oils by Conversion to Mono-Esters and Blending with Diesel Oil or Alcohols*; SAE Technical Papers; SAE International: Warrendale, PA, USA, 1984.

29. Vellguth, G. *Performance of Vegetable Oils and Their Monoesters as Fuels for Diesel Engines*; SAE Technical Papers; SAE International: Warrendale, PA, USA, 1983.

30. De Almeida, S.C.A.; Rodrigues Belchior, C.; Nascimento, M.V.G.; Dos, L.; Vieira, S.R.; Fleury, G. Performance of a diesel generator fuelled with palm oil. *Fuel* **2002**, *81*, 2097–2102. [CrossRef]

31. Graboski, M.S.; McCormick, R.L. Combustion of fat and vegetable oil derived fuels in diesel engines. *Prog. Energy Combust. Sci.* **1998**, *24*, 125–164. [CrossRef]

32. Kim, J.-K.; Jeon, C.-H.; Lee, H.W.; Park, Y.-K.; Min, K.-I.; Hwang, I.-H.; Kim, Y.-M. Effect of Accelerated High Temperature on Oxidation and Polymerization of Biodiesel from Vegetable Oils. *Energies* **2018**, *11*, 3514. [CrossRef]

33. Zahan, K.A.; Kano, M. Biodiesel Production from Palm Oil, Its By-Products, and Mill Effluent: A Review. *Energies* **2018**, *11*, 2132. [CrossRef]

34. Tesfa, B.; Gu, F.; Mishra, R.; Ball, A. Emission characteristics of a ci engine running with a range of biodiesel feedstocks. *Energies* **2014**, *7*, 334–350. [CrossRef]

35. Birzietis, G.; Pirs, V.; Dukulis, I.; Gailis, M. Effect of commercial diesel fuel and hydrotreated vegetable oil blend on automobile performance. *Agron. Res.* **2017**, *15*, 964–970.

36. Douvartzides, S.L.; Charisiou, N.D.; Papageridis, K.N.; Goula, M.A. Green diesel: Biomass feedstocks, production technologies, catalytic research, fuel properties and performance in compression ignition internal combustion engines. *Energies* **2019**, *12*, 809. [CrossRef]

37. Murayama, T.; Fujiwara, Y.; Noto, T. Evaluating waste vegetable oils as a diesel fuel. *Proc. Inst. Mech. Eng. Part D J. Automob. Eng.* **2000**, *214*, 141–148. [CrossRef]

38. Appavu, P.; Ramanan, M.V.; Venu, H. Quaternary blends of diesel/biodiesel/vegetable oil/pentanol as a potential alternative feedstock for existing unmodified diesel engine: Performance, combustion and emission characteristics. *Energy* **2019**, *186*, 115856. [CrossRef]

39. Kotek, M.; Mařík, J.; Zeman, P.; Hartová, V.; Hart, J.; Hönig, V. The impact of selected biofuels on the Skoda Roomster 1.4tDi engine's operational parameters. *Energies* **2019**, *12*, 1388. [CrossRef]

40. Babu, V.M.; Murthy, M.K.; Prasad Rao, A.G. Butanol and pentanol: The promising biofuels for CI engines—A review. *Renew. Sustain. Energy Rev.* **2017**, *78*, 1068–1088. [CrossRef]

41. Čedík, J.; Pexa, M.; Holúbek, M.; Aleš, Z.; Pražan, R.; Kuchar, P. Effect of Diesel Fuel-Coconut Oil-Butanol Blends on Operational Parameters of Diesel Engine. *Energies* **2020**, *13*, 3796. [CrossRef]

42. Fukuda, H.; Kondo, A.; Noda, H. Biodiesel fuel production by transesterification of oils. *J. Biosci. Bioeng.* **2001**, *92*, 405–416. [CrossRef]

43. Zaher, F.A.; Soliman, H.M. Biodiesel production by direct esterification of fatty acids with propyl and butyl alcohols. *Egypt. J. Pet.* **2015**, *24*, 439–443. [CrossRef]

44. Laza, T.; Bereczky, Á. Basic fuel properties of rapeseed oil-higher alcohols blends. *Fuel* **2011**, *90*, 803–810. [CrossRef]

45. Valera, H.; Agarwal, A.K. Future Automotive Powertrains for India: Methanol Versus Electric Vehicles. In *Alternative Fuels and Their Utilization Strategies in Internal Combustion Engines*; Springer: Singapore, 2020; pp. 89–123.

46. Patel, S.K.S.; Shanmugam, R.; Kalia, V.C.; Lee, J.K. Methanol production by polymer-encapsulated methanotrophs from simulated biogas in the presence of methane vector. *Bioresour. Technol.* **2020**, *304*, 123022. [CrossRef]

47. Fletcher, J.; Roan, V.; Betts, D. An Investigation of the Feasibility of Coal-Based Methanol for Application in Transportation Fuel Cell Systems. In *Proceedings of the 3rd International Energy Conversion Engineering Conference, San Francisco, CA, USA, 15–18 August 2005*; American Institute of Aeronautics and Astronautics: Reston, VA, USA, 2005; Volume 2, pp. 920–931.

48. Kumabe, K.; Fujimoto, S.; Yanagida, T.; Ogata, M.; Fukuda, T.; Yabe, A.; Minowa, T. Environmental and economic analysis of methanol production process via biomass gasification. *Fuel* **2008**, *87*, 1422–1427. [CrossRef]

49. Gautam, P.; Upadhyay, S.N.; Dubey, S.K. Bio-methanol as a renewable fuel from waste biomass: Current trends and future perspective. *Fuel* **2020**, *273*, 117783. [CrossRef]

50. Verhelst, S.; Turner, J.W.; Sileghem, L.; Vancoillie, J. Methanol as a fuel for internal combustion engines. *Prog. Energy Combust. Sci.* **2019**, *70*, 43–88. [CrossRef]

51. Kumar, D.; Valera, H.; Agarwal, A.K. Numerical Predictions of In-Cylinder Phenomenon in Methanol Fueled Locomotive Engine Using High Pressure Direct Injection Technique. *SAE Tech. Pap. Ser.* **2021**, *1*, 1–15. [CrossRef]

52. Valera, H.; Kumar, D.; Agarwal, A.K. Feasibility Assessment of Methanol Fueling in Two-Wheeler Engine Using 1-D Simulations. *SAE Tech. Pap. Ser.* **2021**, *1*, 1–17. [CrossRef]

53. Çelebi, Y.; Aydın, H. An overview on the light alcohol fuels in diesel engines. *Fuel* **2019**, *236*, 890–911. [CrossRef]

54. Liu, Y.; Jiao, W.; Qi, G. Preparation and properties of methanol–diesel oil emulsified fuel under high-gravity environment. *Renew. Energy* **2011**, *36*, 1463–1468. [CrossRef]

55. Taghavifar, H.; Nemati, A.; Walther, J.H. Combustion and exergy analysis of multi-component diesel-DME-methanol blends in HCCI engine. *Energy* **2019**, *187*, 115951. [CrossRef]

56. Huang, Z.; Lu, H.; Jiang, D.; Zeng, K.; Liu, B.; Zhang, J.; Wang, X. Combustion behaviors of a compression-ignition engine fuelled with diesel/methanol blends under various fuel delivery advance angles. *Bioresour. Technol.* **2004**, *95*, 331–341. [CrossRef] [PubMed]

57. Kumar, S.; Cho, J.H.; Park, J.; Moon, I. Advances in diesel-alcohol blends and their effects on the performance and emissions of diesel engines. *Renew. Sustain. Energy Rev.* **2013**, *22*, 46–72. [CrossRef]

58. Olah, G.A.; Goeppert, A.; Prakash, G.S. *Beyond Oil and Gas: The Methanol Economy*, 3rd ed.; Wiley: Hoboken, NJ, USA, 2018.

59. Kumar, D.; Valera, H.; Gautam, A.; Agarwal, A.K. Simulations of methanol fueled locomotive engine using high pressure co-axial direct injection system. *Fuel* **2021**, *295*, 120231. [CrossRef]

60. Jiao, W.; Wang, Y.; Li, X.; Xu, C.; Liu, Y.; Zhang, Q. Stabilization performance of methanol-diesel emulsified fuel prepared using an impinging stream-rotating packed bed. *Renew. Energy* **2016**, *85*, 573–579. [CrossRef]

61. Rajesh Kumar, B.; Saravanan, S. Use of higher alcohol biofuels in diesel engines: A review. *Renew. Sustain. Energy Rev.* **2016**, *60*, 84–115. [CrossRef]

62. Zhang, C.P.; Zhai, X.M.; Li, Y.J.; Sun, Z.G. Research on Combustion Characteristics and Emissions of Methanol-Diesel Fuel with Different Additives. *Adv. Mater. Res.* **2011**, *354–355*, 462–467. [CrossRef]

63. Venu, H.; Madhavan, V. Influence of diethyl ether (DEE) addition in ethanol-biodiesel-diesel (EBD) and methanol-biodiesel-diesel (MBD) blends in a diesel engine. *Fuel* **2017**, *189*, 377–390. [CrossRef]

64. Jamrozik, A. The effect of the alcohol content in the fuel mixture on the performance and emissions of a direct injection diesel engine fueled with diesel-methanol and diesel-ethanol blends. *Energy Convers. Manag.* **2017**, *148*, 461–476. [CrossRef]

65. Amiri, M.; Shirneshan, A. Effects of air swirl on the combustion and emissions characteristics of a cylindrical furnace fueled with diesel-biodiesel-n-butanol and diesel-biodiesel-methanol blends. *Fuel* **2020**, *268*, 117295. [CrossRef]

66. Huang, J.; Xiao, H.; Yang, X.; Guo, F.; Hu, X. Effects of methanol blending on combustion characteristics and various emissions of a diesel engine fueled with soybean biodiesel. *Fuel* **2020**, *282*, 118734. [CrossRef]

67. Higashide, W.; Li, Y.; Yang, Y.; Liao, J.C. Metabolic engineering of Clostridium cellulolyticum for production of isobutanol from cellulose. *Appl. Environ. Microbiol.* **2011**, *77*, 2727–2733. [CrossRef] [PubMed]

68. Li, H.; Opgenorth, P.H.; Wernick, D.G.; Rogers, S.; Wu, T.Y.; Higashide, W.; Malati, P.; Huo, Y.X.; Cho, K.M.; Liao, J.C. Integrated electromicrobial conversion of CO2 to higher alcohols. *Science* **2012**, *335*, 1596. [CrossRef] [PubMed]

69. da Silva Trindade, W.R.; dos Santos, R.G. 1D modeling of SI engine using n-butanol as fuel: Adjust of fuel properties and comparison between measurements and simulation. *Energy Convers. Manag.* **2018**, *157*, 224–238. [CrossRef]

70. Karabektas, M.; Hosoz, M. Performance and emission characteristics of a diesel engine using isobutanol-diesel fuel blends. *Renew. Energy* **2008**, *34*, 1554–1559. [CrossRef]

71. Ozsezen, A.N.; Turkcan, A.; Sayin, C.; Canakci, M. Comparison of Performance and Combustion Parameters in a Heavy-Duty Diesel Engine Fueled with Iso-Butanol/Diesel Fuel Blends. *Energy Explor. Exploit.* **2011**, *29*, 525–541. [CrossRef]

72. Zheng, Z.; Li, C.; Liu, H.; Zhang, Y.; Zhong, X.; Yao, M. Experimental study on diesel conventional and low temperature combustion by fueling four isomers of butanol. *Fuel* **2015**, *141*, 109–119. [CrossRef]

73. Rajesh Kumar, B.; Saravanan, S. Effects of iso-butanol/diesel and n-pentanol/diesel blends on performance and emissions of a di diesel engine under premixed LTC (low temperature combustion) mode. *Fuel* **2016**, *170*, 49–59. [CrossRef]

74. Mathan Raj, V.; Ganapathy Subramanian, L.R.; Manikandaraja, G. Experimental study of effect of isobutanol in performance, combustion and emission characteristics of CI engine fuelled with cotton seed oil blended diesel. *Alexandria Eng. J.* **2018**, *57*, 1369–1378. [CrossRef]

75. Xiao, H.; Guo, F.; Wang, R.; Yang, X.; Li, S.; Ruan, J. Combustion performance and emission characteristics of diesel engine fueled with iso-butanol/biodiesel blends. *Fuel* **2020**, *268*, 117387. [CrossRef]

76. Venkateswarlu, K.; Murthy, B.S.R.; Subbarao, V.V. *An Experimental Investigation on Performance, Combustion and Emission Characteristics of Diesel—Biodiesel Blends with Isobutanol as an Additive*; SAE Technical Papers; SAE International: Warrendale, PA, USA, 2012.

77. Slovenian Institute for Standardization. *EN 590. Automotive Fuels. Diesel. Requirements and Test Methods*; Slovenian Institute for Standardization: Ljubljana, Slovenia, 2013.

78. German Institute for Standardization (DIN). *EN 14214. Automotive Fuels. Fatty Acid Methyl Esters (FAME) for Diesel Engines. Requirements and Test Methods*; German Institute for Standardization (DIN): Berlin, Germany, 2012.

79. German Institute for Standardization (DIN). *ČSN DIN 51900-1. Testing of Solid and Liquid Fuels—Determination of the Gross Calorific Value by the Bomb Calorimeter and Calculation of the Net Calorific Value—Part 1: General Information, Basic Equipment and Method*; German Institute for Standardization (DIN): Berlin, Germany, 2014.

80. German Institute for Standardization (DIN). *ČSN DIN 51900-2. Testing of Solid and Liquid Fuels—Determination of the Gross Calorific Value by the Bomb Calorimeter and Calculation of the Net Calorific Value—Part 2: Method Using Isoperibol or Static Jacket Calorimeter*; German Institute for Standardization (DIN): Berlin, Germany, 2014.

81. Rakopoulos, D.C.; Rakopoulos, C.D.; Giakoumis, E.G.; Dimaratos, A.M.; Kyritsis, D.C. Effects of butanol–diesel fuel blends on the performance and emissions of a high-speed DI diesel engine. *Energy Convers. Manag.* **2010**, *51*, 1989–1997. [CrossRef]

82. Imtenan, S.; Masjuki, H.; Varman, M.; Rizwanul Fattah, I.; Sajjad, H.; Arbab, M. Effect of n-butanol and diethyl ether as oxygenated additives on combustion–emission-performance characteristics of a multiple cylinder diesel engine fuelled with diesel–jatropha biodiesel blend. *Energy Convers. Manag.* **2015**, *94*, 84–94. [CrossRef]

83. Lujaji, F.; Bereczky, A.; Janosi, L.; Novak, C.; Mbarawa, M. Cetane number and thermal properties of vegetable oil, biodiesel, 1-butanol and diesel blends. *J. Therm. Anal. Calorim.* **2010**, *102*, 1175–1181. [CrossRef]

84. McDonnell, K.; Ward, S.; Leahy, J.J.; McNulty, P. Properties of rapeseed oil for use as a diesel fuel extender. *JAOCS J. Am. Oil Chem. Soc.* **1999**, *76*, 539–543. [CrossRef]

85. Algayyim, S.J.M.; Wandel, A.P.; Yusaf, T.; Hamawand, I. The impact of n-butanol and iso-butanol as components of butanol-acetone (BA) mixture-diesel blend on spray, combustion characteristics, engine performance and emission in direct injection diesel engine. *Energy* **2017**, *140*, 1074–1086. [CrossRef]

86. Atmanli, A.; Ileri, E.; Yüksel, B. Experimental investigation of engine performance and exhaust emissions of a diesel engine fueled with diesel-n-butanol-vegetable oil blends. *Energy Convers. Manag.* **2014**, *81*, 312–321. [CrossRef]

87. Atmanlı, A.; Yüksel, B.; İleri, E. Experimental investigation of the effect of diesel–cotton oil–n-butanol ternary blends on phase stability, engine performance and exhaust emission parameters in a diesel engine. *Fuel* **2013**, *109*, 503–511. [CrossRef]

88. Atmanli, A.; Ileri, E.; Yüksel, B. Effects of higher ratios of n-butanol addition to diesel-vegetable oil blends on performance and exhaust emissions of a diesel engine. *J. Energy Inst.* **2015**, *88*, 209–220. [CrossRef]

89. Ileri, E.; Atmanli, A.; Yilmaz, N. Comparative analyses of n-butanol–rapeseed oil–diesel blend with biodiesel, diesel and biodiesel–diesel fuels in a turbocharged direct injection diesel engine. *J. Energy Inst.* **2016**, *89*, 586–593. [CrossRef]

90. Atmanli, A.; Ileri, E.; Yuksel, B.; Yilmaz, N. Extensive analyses of diesel-vegetable oil-n-butanol ternary blends in a diesel engine. *Appl. Energy* **2015**, *145*, 155–162. [CrossRef]

91. Sharon, H.; Jai Shiva Ram, P.; Jenis Fernando, K.; Murali, S.; Muthusamy, R. Fueling a stationary direct injection diesel engine with diesel-used palm oil–butanol blends—An experimental study. *Energy Convers. Manag.* **2013**, *73*, 95–105. [CrossRef]

92. Zhang, Z.H.; Cheung, C.S.; Chan, T.L.; Yao, C.D. Experimental investigation on regulated and unregulated emissions of a diesel/methanol compound combustion engine with and without diesel oxidation catalyst. *Sci. Total Environ.* **2010**, *408*, 865–872. [CrossRef]

93. Sayin, C.; Ozsezen, A.N.; Canakci, M. The influence of operating parameters on the performance and emissions of a DI diesel engine using methanol-blended-diesel fuel. *Fuel* **2010**, *89*, 1407–1414. [CrossRef]

94. Sayin, C. Engine performance and exhaust gas emissions of methanol and ethanol–diesel blends. *Fuel* **2010**, *89*, 3410–3415. [CrossRef]

95. Emiroğlu, A.O.; Şen, M. Combustion, performance and emission characteristics of various alcohol blends in a single cylinder diesel engine. *Fuel* **2018**, *212*, 34–40. [CrossRef]

96. Lujaji, F.; Kristóf, L.; Bereczky, A.; Mbarawa, M. Experimental investigation of fuel properties, engine performance, combustion and emissions of blends containing croton oil, butanol, and diesel on a CI engine. *Fuel* **2011**, *90*, 505–510. [CrossRef]

97. Jamrozik, A.; Tutak, W.; Pyrc, M.; Gruca, M.; Kočiško, M. Study on co-combustion of diesel fuel with oxygenated alcohols in a compression ignition dual-fuel engine. *Fuel* **2018**, *221*, 329–345. [CrossRef]

98. Cogliano, V.J.; Baan, R.; Straif, K.; Grosse, Y.; Lauby-Secretan, B.; El Ghissassi, F.; Bouvard, V.; Benbrahim-Tallaa, L.; Guha, N.; Freeman, C.; et al. Preventable Exposures Associated with Human Cancers. *J. Natl. Cancer Inst.* **2011**, *103*, 1827–1839. [CrossRef]

99.   Wei, H.; Yao, C.; Pan, W.; Han, G.; Dou, Z.; Wu, T.; Liu, M.; Wang, B.; Gao, J.; Chen, C.; et al. Experimental investigations of the effects of pilot injection on combustion and gaseous emission characteristics of diesel/methanol dual fuel engine. *Fuel* **2016**, 427–441. [CrossRef]

100. Wei, L.; Yao, C.; Wang, Q.; Pan, W.; Han, G. Combustion and emission characteristics of a turbocharged diesel engine using high premixed ratio of methanol and diesel fuel. *Fuel* **2015**, *140*, 156–163. [CrossRef]

101. Holúbek, M.; Cedík, J.; Vu, H.; Pexa, M. Influence of diesel—Butanol fuel blends on production of solid particles by CI engine. In Proceedings of the TAE 2019—7th International Conference on Trends in Agricultural Engineering 2019, Prague, Czech Republic, 17–20 September 2019; pp. 171–176.

102. Geng, L.; Chen, Y.; Chen, X.; Lee, C. fon F. Study on combustion characteristics and particulate emissions of a common-rail diesel engine fueled with n-butanol and waste cooking oil blends. *J. Energy Inst.* **2019**, *92*, 438–449. [CrossRef]

103. Zhang, Z.-H.; Balasubramanian, R. Influence of butanol addition to diesel–biodiesel blend on engine performance and particulate emissions of a stationary diesel engine. *Appl. Energy* **2014**, *119*, 530–536. [CrossRef]

104. Agarwal, A.K.; Sharma, N.; Singh, A.P.; Kumar, V.; Satsangi, D.P.; Patel, C. Adaptation of Methanol–Dodecanol–Diesel Blend in Diesel Genset Engine. *J. Energy Resour. Technol.* **2019**, *141*, 102203. [CrossRef]

105. Holúbek, M.; Pexa, M.; Čedík, J.; Mader, D. Effect of long-term operation of combustion engine running on n-butanol—Rapeseed oil—Diesel fuel blend. *Agron. Res.* **2019**, *17*, 1001–1012. [CrossRef]

106. Holubek, M.; Pexa, M.; Pavlu, J.; Cedík, J.; Vesela, K.; Kuchar, P. Analysis of the Influence of Fuel on Oil Charge and Engine Wear. *Manuf. Technol.* **2019**, *19*, 64–70. [CrossRef]